Received: 7 November 2017 | Accepted: 19 February 2018

DOI: 10.1111/gcb.14164

PRIMARY RESEARCH ARTICLE

WILEY Global Change Biology

Hydraulic redistribution affects modeled carbon cycling via soil microbial activity and suppressed fire

Congsheng Fu[1] | Guiling Wang[1] | Kenneth Bible[2] | Michael L. Goulden[3] | Scott R. Saleska[4] | Russell L. Scott[5] | Zoe G. Cardon[6]

[1]Department of Civil & Environmental Engineering, Center for Environmental Science and Engineering, University of Connecticut, Storrs, Connecticut

[2]Forest Service, Pacific Northwest Research Station, Portland, Oregon

[3]Department of Earth System Science, University of California, Irvine, California

[4]Department of Ecology and Evolutionary Biology, University of Arizona, Tucson, Arizona

[5]Southwest Watershed Research Center, USDA-Agricultural Research Service, Tucson, Arizona

[6]The Ecosystems Center, Marine Biological Laboratory, Woods Hole, Massachusetts

Correspondence
Zoe G. Cardon, The Ecosystems Center, Marine Biological Laboratory, Woods Hole, MA.
Email: zcardon@mbl.edu
and
Guiling Wang, Department of Civil & Environmental Engineering, and Center for Environmental Science and Engineering, University of Connecticut, Storrs, CT.
Email: guiling.wang@uconn.edu

Present address
Congsheng Fu, Key Laboratory of Watershed Geographic Sciences, Nanjing Institute of Geography and Limnology, Chinese Academy of Sciences, Nanjing, China.

Funding information
U.S. Department of Energy, Biological and Environmental Research, Grant/Award Number: DE-SC0008182 ER65389

Abstract

Hydraulic redistribution (HR) of water from moist to drier soils, through plant roots, occurs world-wide in seasonally dry ecosystems. Although the influence of HR on landscape hydrology and plant water use has been amply demonstrated, HR's effects on microbe-controlled processes sensitive to soil moisture, including carbon and nutrient cycling at ecosystem scales, remain difficult to observe in the field and have not been integrated into a predictive framework. We incorporated a representation of HR into the Community Land Model (CLM4.5) and found the new model improved predictions of water, energy, and system-scale carbon fluxes observed by eddy covariance at four seasonally dry yet ecologically diverse temperate and tropical AmeriFlux sites. Modeled plant productivity and microbial activities were differentially stimulated by upward HR, resulting at times in increased plant demand outstripping increased nutrient supply. Modeled plant productivity and microbial activities were diminished by downward HR. Overall, inclusion of HR tended to increase modeled annual ecosystem uptake of CO_2 (or reduce annual CO_2 release to the atmosphere). Moreover, engagement of CLM4.5′s ground-truthed fire module indicated that though HR increased modeled fuel load at all four sites, upward HR also moistened surface soil and hydrated vegetation sufficiently to limit the modeled spread of dry season fire and concomitant very large CO_2 emissions to the atmosphere. Historically, fire has been a dominant ecological force in many seasonally dry ecosystems, and intensification of soil drought and altered precipitation regimes are expected for seasonally dry ecosystems in the future. HR may play an increasingly important role mitigating development of extreme soil water potential gradients and associated limitations on plant and soil microbial activities, and may inhibit the spread of fire in seasonally dry ecosystems.

KEYWORDS
decomposition, heterotrophic respiration, hydraulic descent, hydraulic lift, hydraulic redistribution, NEE, nutrient limitation

1 | INTRODUCTION

In seasonally dry ecosystems, when gradients in water content develop in the soil column, plant root systems can serve as conduits for water flow from moist to dry soil along the water potential gradient. This "hydraulic redistribution" (HR) of water can be upward during dry periods as "hydraulic lift" (Richards & Caldwell, 1987), downward during rainy periods as "hydraulic descent" (Ryel,

Caldwell, Leffler, & Yoder, 2003), or lateral (Brooks, Meinzer, Coulombe, & Gregg, 2002). The effects of HR on plant physiology and landscape hydrology have now been amply demonstrated in seasonally dry ecosystems worldwide (Neumann & Cardon, 2012; Prieto, Armas, & Pugnaire, 2012; Sardans & Peñuelas, 2014). During dry seasons, between two and eighty percent (multi-ecosystem average ~15%) of transpiration during daytime is supplied by upward HR the previous night (Neumann & Cardon, 2012). Enhanced transpiration is supported by increased stomatal opening, which can also enhance photosynthesis. A number of modeling studies have now built on this plant perspective to explore the impact of HR on surface water and energy budgets (Baker et al., 2009; Domec et al., 2010; Fu et al., 2016; Luo, Liang, & McCarthy, 2013; Quijano & Kumar, 2015; Wang, 2011), ecosystem carbon balance (e.g., Baker et al., 2009; Domec et al., 2010; Luo et al., 2013), and plant community composition (e.g., Barron-Gafford et al., 2017; Wang, Alo, Mei, & Sun, 2011; Yu & D'Odorico, 2015).

At the ecosystem scale, however, it is the balance of net photosynthetic plant carbon gain with carbon loss through decomposition and fire that sets whether carbon is taken up from or lost to the atmosphere from seasonally dry ecosystems. HR's capacity to affect microbial activity, decomposition, nutrient availability to plants, and soil respiration rates in the field have long been suspected (e.g., Aanderud & Richards, 2009; Caldwell, Dawson, & Richards, 1998) and have recently been confirmed in sagebrush steppe (e.g., Cardon, Stark, Herron, & Rasmussen, 2013). HR can therefore affect system scale carbon cycling and land-atmosphere carbon dioxide (CO_2) exchange through at least two biological pathways (Figure 1). HR can influence plant physiology, for example, enhancing stomatal conductance during drought and thus increasing photosynthesis (green shading, Figure 1). HR can also affect soil microbial activity, the magnitude of heterotrophic soil respiration, and nutrient cycling and availability for plant growth (brown shading, Figure 1). The two interacting biological pathways shown in Figure 1 have not previously been integrated into one HR modeling framework, and their relative strengths in affecting primary productivity remains unknown. Furthermore, fire ignited through human activities or lightning can be a major driver of the ecology of seasonally dry ecosystems, and fire's effects on CO_2 fluxes potentially swamp plant and microbial controls over CO_2 fluxes to the atmosphere (Frank et al., 2015). The potential influence of HR on carbon loss via fire in seasonally dry ecosystems has not been previously explored using modeling, though upward HR maintains plant hydration and moistens upper soil layers most strongly during dry seasons, the very time when fire can spread and dominate ecosystem carbon loss.

Here, we used a combination of modeling and eddy flux measurements to examine the strength and interplay of plant and microbial pathways influenced by HR (Figure 1). We worked in ecologically diverse, seasonally dry temperate and tropical ecosystems arrayed from Washington State to the Amazon, with annual rainfall spanning ~400–2,000 mm, soils ranging from clay to sandy loam and loamy sand, and diverse vegetation types. HR has previously been detected at AmeriFlux sites within these diverse

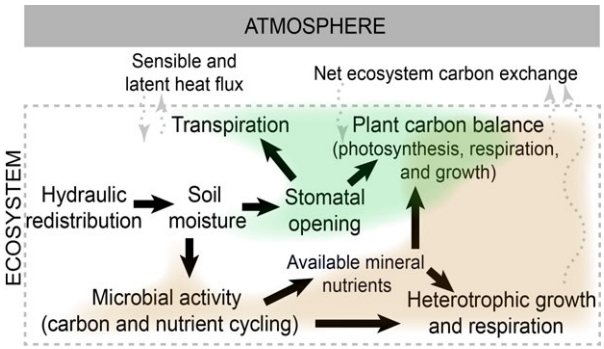

FIGURE 1 Plant (green shading) and microbial (brown shading) pathways through which soil moisture, altered by hydraulic redistribution, affects ecosystem element cycling as well as carbon and energy exchange with the atmosphere

ecosystems: US-Wrc (Wind River Crane, Pacific Northwest douglas fir/hemlock forest, WA); US-SCf (Southern California Climate Gradient, oak-pine forest, CA); US-SRM (Santa Rita Mesquite, semidesert grassland with encroached mesquite, AZ); and BR-Sa1 (Santarem KM67, evergreen broadleaf primary tropical forest, Brazil). We incorporated Ryel, Caldwell, Yoder, Or, and Leffler (2002) formulation of HR into the Community Land Model with Century-based representation of soil carbon pool kinetics (Oleson et al., 2013), and first checked whether including HR improved the match between modeled and measured evapotranspiration, Bowen ratio, and net ecosystem exchange of CO_2 with the atmosphere (NEE), when compared to the default CLM4.5 modeling scheme. We then explored how changes in soil moisture associated with both upward and downward HR affected interlinked plant and microbial pathways driving ecosystem carbon and nutrient cycling (Figure 1), and we examined whether HR-associated changes in surface soil moisture and fuel availability were sufficiently large to affect the incidence and spread of modeled fire and associated large carbon fluxes to the atmosphere.

2 | MATERIALS AND METHODS

2.1 | AmeriFlux sites

Sites US-Wrc, US-SCf, US-SRM, and BR-Sa1 were chosen for several reasons. HR has been detected at all four, via sap-flow and/or soil moisture measurements (Kitajima, Allen, & Goulden, 2013; Meinzer et al., 2004; Oliveira, Dawson, Burgess, & Nepstad, 2005; Scott, Cable, & Hultine, 2008). The sites are all seasonally dry but otherwise ecologically diverse (Table 1, http://ameriflux.lbl.gov/sites/). The sites offer concurrent meteorological forcing, soil moisture, latent and sensible heat flux, and NEE data essential for modeling and model-measurement comparisons. Empirical data for US-SRM, US-SCf, and BR-Sa1 were downloaded from the AmeriFlux data repository (http://ameriflux.lbl.gov/data/data-availability/, accessed 6/20/2016, 6/30/2016, and 7/6/2016, respectively); data for US-SCf were downloaded from http://www.ess.uci.edu/~california/ (accessed 8/31/2016).

TABLE 1 Study site information

Site	Location	Elevation (m)	Köppen climate	Vegetation	Annual precipitation (mm)	Average temperature (°C)	Atmospheric forcing data
US-SCf	33.8080°N, 116.7717°W, CA	1,710	Mediterranean (Csa)	Oak/pine forest	530[a]	13.3[a]	2007–2012
BR-Sa1	2.8566°S, 54.9589°W, Pará, Brazil	88	Tropical monsoon (Am)	Macaranduba, Jatoba, Taxi	1,910[b]	25.0[b]	2009–2011
US-Wrc	45.8205°N, 121.9519°W, WA	371	Mediterranean (Csb)	Douglas fir, western hemlock	2,220[c]	8.7[c]	1999–2008
US-SRM	31.8214°N, 110.8661°W, AZ	1,116	Cold semi-arid (BSk)	Mesquite trees, bunchgrass	380[d]	19.6[e]	2004–2012

[a]2007–2012.
[b]From Grant et al. (2009).
[c]1978–1998 from NOAA station 5 km north of the US-Wrc tower.
[d]1937–2007 from Scott, Jenerette, Potts, and Huxman (2009).
[e]2004–2012.

2.2 | CLM4.5 modeling framework

The Community Land Model Version 4.5 (CLM4.5 public release, Oleson et al., 2013), with Century-based soil carbon pool kinetics, was used to simulate surface water and energy budgets at the land surface, carbon and nitrogen biogeochemistry, plant phenology, vegetation growth, and mortality. CLM4.5 supports tracking the distribution and dynamics of soil organic carbon and water vertically throughout the soil column—essential for modeling and quantifying the integrated effects of HR that by nature are differentially distributed vertically. At BR-Sa1, maximum soil depth was increased to 12 m following field observations and common modeling practice (Table 2; Baker et al., 2009; Grant et al., 2009; Ivanov et al., 2012; Lee, Oliveira, Dawson, & Fung, 2005; Nepstad et al., 1994; Zheng & Wang, 2007). Table S1 provides Clapp and Hornberger (1978) *"B"* factors for all soil layers at each site. At US-Wrc, *"B"* factors were shifted slightly relative to values used in our previous modeling (see Supporting Information), but still within ranges of *B* observed for the observed texture profiles (Fu et al., 2016).

Vegetation in CLM4.5 is represented as a combination of plant functional types (PFTs); all vegetation-related state variables and surface fluxes are solved at the PFT level. Realistic simulation of leaf area index (LAI) is critical, as LAI controls the surface energy, water, and carbon budgets and links vegetation's biogeophysical and biogeochemical processes. In CLM4.5, LAI is estimated based on the leaf carbon storage and the specific leaf area at the canopy top (SLA), but SLA can vary significantly among species within the same PFT. To represent the specific plant species observed at each site more realistically, the SLA for broadleaf deciduous shrubs at US-Wrc site and for all woody PFTs at the US-SCf site was reduced to 1/3 of the default values set for global applications of CLM4.5. These modified values were within the scopes of SLA for the corresponding species (Reich, Walters, & Ellsworth, 1997). CLM4.5 simulates plant phenology reasonably well (Table S2, Supporting Information; Thornton et al., 2002), except at the driest site US-SRM, where the model predicts multiple successive rounds of leaf production and abscission within single years (Figure S1). To avoid this problem, we constrained the leaf phenology at US-SRM based on observations.

2.3 | Modeling HR

We incorporated the HR scheme from Ryel et al. (2002) into CLM4.5. Soil water moved via plant roots between any two soil layers (HR), in addition to the default flux already in CLM4.5 between adjacent soil layers through soil pore space. We quantified the HR-associated soil water flux q_{HR}(i, j) (cm/hr) between a receiving soil layer *i* and a giving soil layer *j* as:

$$q_{\mathrm{HR}}(i,j) = -C_{\mathrm{RT}}\Delta\varphi_{\mathrm{m}}c_{\mathrm{j}}\frac{F_{\mathrm{root}}(i)F_{\mathrm{root}}(j)}{1-F_{\mathrm{root}}(j)} \quad (1)$$

C_{RT} is the maximum radial soil-root conductance (cm MPa^{-1} hr^{-1}), $\Delta\varphi_m$ is water potential difference between two soil layers (MPa), F_{root} (*i*) is root fraction in layer *i*, and the factor reducing soil-root conductance for water in the giving layer c_j is

$$c_{\mathrm{j}} = \frac{1}{1+\left(\frac{\varphi_{\mathrm{j}}}{\varphi_{50}}\right)^{\mathrm{b}}} \quad (2)$$

In Equation (2), φ_j is soil water potential in layer *j* (MPa), φ_{50} is the soil water potential where soil-root conductance is reduced by 50% (MPa), and *b* is an empirical constant. Our previous work (Fu et al., 2016) illustrated that CLM modeling results were relatively sensitive to variations in C_{RT} and φ_{50}, and were relatively insensitive to variations in the parameter b. Here, we used φ_{50} and b as in (Li, Wang et al., 2012; Ryel et al., 2002; Zheng & Wang, 2007). We set C_{RT} to 0.1 at the three forest sites, consistent with Ryel et al. (2002), but tuned C_{RT} to 1.0 at US-SRM to better capture the diel fluctuations in soil moisture during dry periods.

2.4 | Experimental design

To derive a stable vertical soil carbon distribution for initial conditions, we used an accelerated decomposition spinup run of 1,200 years followed by a normal spinup run of 2,100 years that

TABLE 2 Data sources for model inputs

Site	Atmospheric forcing data	Land coverage	Maximum soil depth	Soil texture	Root fraction profile
US-SCf	M. Goulden[a]	Table 3 in Anderson and Goulden (2011), "Doak"	3.8 m (Default)	Sandy loam, loamy sand[b]	Jackson et al. (1996)
BR-Sa1	S. Saleska[c]	NCAR database (broadleaf evergreen tree: 84%; broadleaf deciduous tree: 10%; grass: 6%)	12 m, Nepstad et al. (1994)	Clay. Table 1 in Grant et al. (2009)	Figure 2, Ivanov et al. (2012)
US-Wrc	AmeriFlux tower data[d]	Google Earth map; Table 2 in Shaw et al. (2004) (overstory trees: 24%; vine maple: 36%; salal and oregon grape: 40%)	3.8 m (Default)	Sandy loam, with loam and clay loam. Figure 4 in Warren, Meinzer, Brooks, & Domec (2005)	Jackson et al. (1996)
US-SRM	AmeriFlux tower data[e]	R. Scott, USDA-ARS (bare ground: 40%; mesquite canopy: 35%; grass: 25%)	3.8 m (Default)	Loamy sand[f]. Scott et al. (2009)	Jackson et al. (1996)

[a]http://www.ess.uci.edu/~california/, accessed 6/29/2013.
[b]M. Goulden (pers. comm.)
[c](pers.comm.)
[d]ftp://cdiac.ornl.gov/pub/ameriflux/data/Level2/Sites_ByName/Wind_River_Field_Station/with_gaps/, accessed 7/5/2013.
[e]ftp://cdiac.ornl.gov/pub/ameriflux/data/Level2/Sites_ByName/Santa_Rita_Mesquite_Savanna/with_gaps/, accessed 4/2/2013.
[f]ftp://cdiac.ornl.gov/pub/ameriflux/data/Level1/Sites_ByName/Santa_Rita_Mesquite_Savanna/biological_data/SantaRitaMesquite_Biological_Data_Version2_7Nov2008.xls, accessed 3/29/2013.

cycled through the site-specific meteorological forcing multiple times (Oleson et al., 2013). HR was included during this spinup, because it is known to occur at all four sites. The carbon and nitrogen pools resulting from this spinup were used to initialize subsequent modeling runs.

Simulations using the CLM4.5 modeling scheme including HR are referred to as "CLM4.5+HR". At each AmeriFlux site, we first checked whether CLM4.5+HR improved the match between measured and modeled net ecosystem carbon exchange with the atmosphere (NEE), evapotranspiration (ET), and the Bowen ratio, when compared to the default CLM4.5 modeling scheme lacking explicit representation of HR ("CLM4.5noHR" also referred to as "noHR"). We then used both models to explore how changes in soil moisture associated with HR affected plant production, heterotrophic respiration, nutrient mineralization, nutrient availability, and biosphere-atmosphere CO_2 exchange.

We developed a "CLM4.5hybrid" modeling approach to explore the relative strengths of HR's effects exerted through the plant and microbial pathways (Figure 1, and see Supporting Information). Briefly, in the "CLM4.5hybrid" simulations, HR affected soil moisture distribution for all modeled processes *except* for those soil microbial processes that are explicitly affected by soil moisture content in core CLM4.5 equations: decomposition, nitrification, and denitrification. (Calculation of microbial immobilization of nutrients is not directly affected by soil water content in CLM4.5.) Decomposition, nitrification, and denitrification rates in the CLM4.5hybrid simulation were driven using soil moisture output from the CLM4.5noHR run, effectively making them blind to HR. By comparing results from the CLM4.5hybrid, CLM4.5+HR and CLM4.5noHR runs, we could assess the relative importance of effects of HR initiated through the plant pathway alone (CLM4.5hybrid vs CLM4.5noHR) vs those initiated through both the plant and microbial pathways (CLM4.5+HR vs CLM4.5noHR).

Finally, we examined whether HR could affect the frequency or extent of fire by taking advantage of the fire module developed in CLM4.5 (Li, Levis, & Ward, 2013; Li, Zeng, & Levis, 2012). By running the CLM4.5+HR and the default CLM4.5noHR simulations with the fire module engaged (referred to as "CLM4.5+HR" and "CLM4.5noHR+fire"), we explored whether HR-associated changes in surface soil moisture and fuel availability were sufficiently large to affect the incidence and spread of modeled fire and associated large carbon fluxes to the atmosphere.

3 | RESULTS

3.1 | Comparison of predicted and measured ecosystem process

Weekly means were calculated at each AmeriFlux site from multi-year simulations and from measured eddy flux datasets. Root mean square error (RMSE), quantifying the disagreement between modeled and measured Bowen ratio, ET, and NEE, is smaller when HR is included in CLM4.5 (Table 3). At US-Wrc, including HR in CLM4.5 improved the match of *mean* modeled and measured ET, but the match of dynamics around the mean was not improved and drove higher RMSE for ET (see Supporting Information). Taylor plots (Taylor, 2001) (Figure S2) show that inclusion of HR at all sites improves model-measurement match quantified by several statistical metrics.

TABLE 3 Root mean square error (RMSE) quantifying disagreement between modeled and measured weekly mean Bowen ratio (B), ET, and NEE, for the CLM4.5+HR and CLM4.5noHR simulations

	US-SCf	BR-Sa1	US-Wrc	US-SRM
B (+HR)	4.52	0.11	2.87	6.72
B (noHR)	10.16	0.21	2.98	34.67
ET (+HR)	0.62	0.26	0.80	0.28
ET (noHR)	0.85	0.41	0.75	0.34
NEE (+HR)	1.97	1.22	1.98	0.67
NEE (noHR)	2.23	1.32	2.07	0.74

Time courses of measured and modeled ET and NEE are shown in Figures S3 and S4. Modeled gross primary production, net primary production, and soil organic carbon content compare reasonably with published literature values in Table 4. Modeled and observed maximum LAI (Aragão, Shimabukuro, Espírito Santo, & Williams, 2005; Fellows & Goulden, 2013; Scott, Biederman, Hamerlynck, & Barron-Gafford, 2015), liter mass, fine root biomass, and leaf expansion dates (Richardson et al., 2012) are compared in Table S2.

3.2 | Carbon and nutrient cycling

The timing of upward and downward HR is predictable from seasonal dry spells and rain patterns. Figure 2a shows the multiyear average instantaneous gain (blue) and loss (gold) of water moved exclusively by HR among different soil layers in the CLM4.5+HR simulation. Soil moisture is quantified as volumetric soil moisture content (%). The cumulative effects of HR over time on soil moisture through all system processes (e.g., including through altered plant biomass and/or transpiration) is quantified as the difference in modeled soil moisture between the CLM4.5+HR and CLM4.5noHR simulations (Figure S5a). This differential soil moisture caused by HR persisted throughout most of the year and its effects cascaded through ecosystem processes, altering modeled nitrogen (N)- and carbon (C)-cycling (Figure 2b,c). (Figure S5b,c shows the modeled pools and rates which were used to derive the differences between the CLM4.5+HR and CLM4.5noHR runs shown in Figure 2b,c).

During dry seasons (designated with yellow blocks, Figure 2b, c), upward HR at all four sites increased modeled gross N mineralization from organic matter (19%, 9%, 12%, and 8% increase, respectively, at US-SCf, BR-Sa1, US-Wrc, and US-SRM), microbial N immobilization (17%, 10%, 6%, and 22%, respectively), and plant mineral N uptake (43%, 10%, 18%, and 91%, respectively), relative to simulated rates without HR (Figures 2b and S5b). This increase in modeled plant mineral N uptake was driven by increased plant demand associated with increased dry season gross primary productivity (43%, 11%, 19%, and 54%, respectively, Figures 2c and S5c). Upward HR also, however, increased dry season heterotrophic respiration of CO_2 by soil microbes (19%, 10%, 19%, and 15% respectively, Figures 2c and S5c, and as suggested in Figure 1). The overall effect of upward HR on the modeled system-level carbon balance was, therefore, complex. At US-SRM, dry season NEE was positive, indicating release of CO_2 to the atmosphere occurred whether HR was included in the modeling or not (Figure S5; Table 5). However, upward HR at US-SRM reduced that modeled dry season loss of CO_2 to the atmosphere by 29% relative to the simulation without HR (Figure 2c; Table 5). At the other three sites, modeled NEE was negative overall during the dry season (Figure S5c; Table 5), indicating net CO_2 uptake from the atmosphere. Upward HR enhanced modeled dry season CO_2 uptake by 100% at US-SCf and 21% at US-Wrc (Figure 2c; Table 5).

TABLE 4 Observed and mean (±*SD*) modeled (CLM4.5+HR) gross and net primary production (GPP and NPP, gC m^{-2} $year^{-1}$) and soil organic carbon content (SOC, kgC m^{-2}). Values in brackets are ranges of observations. Modeling data were extracted for time spans matching observational data

	US-SCf		BR-Sa1		US-Wrc		US-SRM	
	Observed	Modeled	Observed	Modeled	Observed	Modeled	Observed	Modeled
GPP	1,086 ± 111[a]	1,365 ± 62	3,160[b]	2,970 ± 133	1,378[c]	1,613 ± 78	280[d] [~210–315]	234 ± 20
NPP	–	569 ± 29	900[e]	1,033 ± 84	597[f]	630 ± 49	–	100 ± 15
SOC (0–20 cm)	–	7.3 ± 0.003	–	6.5 ± 0.005	6.5 [0.9–24][g]	7.1 ± 0.003	1.05[g], 1.9[h]	0.8 ± 0.001
SOC (0–1 m)	–	18.1 ± 0.004	2–18 [mode 9][i]	14.2 ± 0.007	–	17.8 ± 0.003	5.3[h]	2.3 ± 0.001

[a]From Fellows & Goulden (2013), years 2007–2009.
[b]From Hutyra et al. (2008), years 2003–2005.
[c]From Falk, Wharton, Schroeder, Ustin, & Paw U (2008), years 1999–2004.
[d]From Scott et al. (2009), years 2004–2007, and for 2004–2015, 331 ± 75, R. Scott pers. comm.
[e]From Chambers et al. (2014), for central Amazonian forests.
[f]From Harmon et al. (2004).
[g]From biological data files, accessed August 2015, ftp://cdiac.ornl.gov/pub/ameriflux/data/Level1/.
[h]R. Scott pers. comm.
[i]From Koven et al. (2013), for tropical latitudes.

Downward HR also affected modeled C- and N-cycling. Downward HR was dominant at US-SRM (Figure 2a), where total annual rainfall was low but concentrated in approximately 2 months after the dry season (Figure S6a). Not surprisingly, measurements and modeling showed that rainfall strongly stimulated plant and microbial processes (Figure S5). Modeling indicated that the extent of stimulation was curtailed, however, by downward HR. This was because downward HR moved rain from surface layers (where substrates for decomposition and plant root density are maximum) to drier deeper soil layers (where litter and plant roots are more sparse). Downward HR led to decreased modeled gross mineralization, microbial N immobilization, and plant mineral N uptake during July and August, relative to the no HR case (16%, 13%, and 27% decreases, respectively, Figures 2b and S5b). Downward HR also led to decreased modeled GPP and heterotrophic respiration during July and August, relative to the noHR case (17% and 15% decreases, respectively, Figures 2c and S5c). The overall effect of downward HR on modeled NEE during July and August at US-SRM was a 37% decrease in ecosystem carbon uptake from the atmosphere relative to the noHR case (Figures 2c and S5c).

Evaluating the combined effect of upward and downward HR on annual NEE at each site therefore required integrating throughout the year (Table 5). At US-SRM, inclusion of HR in CLM4.5 caused modeled annual NEE to shift to 19% stronger annual ecosystem uptake of CO_2 from the atmosphere. At US-SCf, modeled annual net CO_2 release to the atmosphere in CLM4.5+HR was 93% lower than in CLM4.5noHR, largely because upward HR spurred a notable increase in CO_2 uptake during the dry season. At US-Wrc, including HR changed the annual NEE from net annual ecosystem release of CO_2 to the atmosphere (in CLM4.5noHR) to net annual uptake of CO_2 (in CLM4.5+HR), driven by changes in NEE during both dry and wet seasons. At BR-Sa1, small HR-induced changes in modeled NEE in the dry and wet seasons offset one another, resulting in modeled annual NEE being indistinguishable with and without HR.

3.3 | Carbon pools in vegetation, litter, and coarse woody debris

Interannual mean (±*SE*) vegetative structural carbon pools were larger in CLM4.5+HR than in CLM4.5noHR simulations, at all four sites (Figure 3). Only one component of vegetation—the fine root pool at US-SRM—was reduced when HR was included in CLM4.5. Inclusion of HR drove decreased coarse woody debris at US-SCf, BR-Sa1, and US-Wrc, and increased litter C at US-SCf and US-SRM. Soil organic carbon pools were large (Table 4); in the short time frame of our comparative modeling they did not change significantly.

3.4 | Plant- and microbe-driven pathways

The "CLM4.5hybrid" model distinguished effects of HR initiated through the plant pathway alone (shaded green, Figure 1). CLM4.5+HR simulations, in contrast, captured the multiple effects of HR on both plants and microbes (Figure 1, green and brown shading). Panels in Figure 4b illustrate modeled process rates (per m^2 land surface) produced by the CLM4.5+HR (blue), CLM4.5hybrid (green), and CLM4.5noHR (red) simulations. Data from simulations during 1 year only are presented to ease visual comparisons among modeling runs. Panels are similar to those in Figure S5b,c, but with the addition of modeled nutrient limitation of GPP. This nutrient limitation was quantified as the % reduction in potential GPP caused by unfulfilled plant N demand. GPP panels show both the modeled potential (pastel lines) and realized GPP (solid lines).

During the dry season at all sites (yellow blocks, Figure 4b), modeled microbial heterotrophic respiration and gross mineralization were most similar in the CLM4.5noHR (red) and CLM4.5hybrid (green) cases. This was expected; the two simulations shared the CLM4.5noHR soil moisture driver, so the green and red traces for those two microbial processes largely overlap during the dry season (Figure 4b). Modeled GPP during dry seasons, however, was most similar between the CLM4.5hybrid (green) and CLM4.5+HR (blue) runs (Figure 4b). (The two runs shared HR's effects on GPP via the plant pathway.) Therefore, GPP in the CLM4.5hybrid run (green) at US-SCf, BR-Sa1, and US-Wrc was stimulated (via the plant pathway) by upward HR relative to the noHR (red) run, but gross mineralization was not. The result was increased modeled nutrient limitation of GPP during the dry season at US-SCf, BR-SA1, and US-Wrc in both the CLM4.5hybrid (green) and CLM4.5+HR (blue) runs, compared to the CLM4.5noHR run (red) (Figure 4b). At US-SRM, in contrast, highest GPP and strong hydraulic descent occurred when rains returned just after the dry season. Modeled gross mineralization of N by soil microbes was highest in the CLM4.5noHR and CLM4.5hybrid cases (Figure 4b) because without downward HR, surface soil (where root density and detritus availability are high) remained more moist during the rainy season. Early in the rainy season, potential GPP was highest in the CLM4.5noHR case (with most moist surface soils), but realized GPP rapidly diminished when nutrient limitation emerged approximately Julian day 210.

For all sites, the lowermost scatterplot panels of Figure 4b illustrate the calculated stimulation, or diminution, of GPP by HR attributable to the plant pathway. The scatterplot panel for each site focuses on the time period during which the three simulations' predictions of realized GPP most diverge. For the three sites with strong hydraulic lift, divergence is dominantly during the dry season. At US-SCf, ~80% of the HR-related stimulation of GPP (above the CLM4.5noHR value) could be explained by the plant pathway alone, independent of any soil moisture effect on decomposition. Similarly at US-Wrc, much of the stimulation of GPP could be explained via effects on the plant pathway. At BR-Sa1, the three models did not diverge strongly, but less than half of the small HR-related stimulation of GPP could be explained by the plant pathway alone.

At US-SRM, differences among models in GPP were most obvious during hydraulic descent driven by rains in July and August (Figure 4b). We therefore examined modeled diminution (rather than stimulation) of GPP attributable to plant and microbial pathways. During a short early period of maximum modeled GPP on ~Julian day 210, the

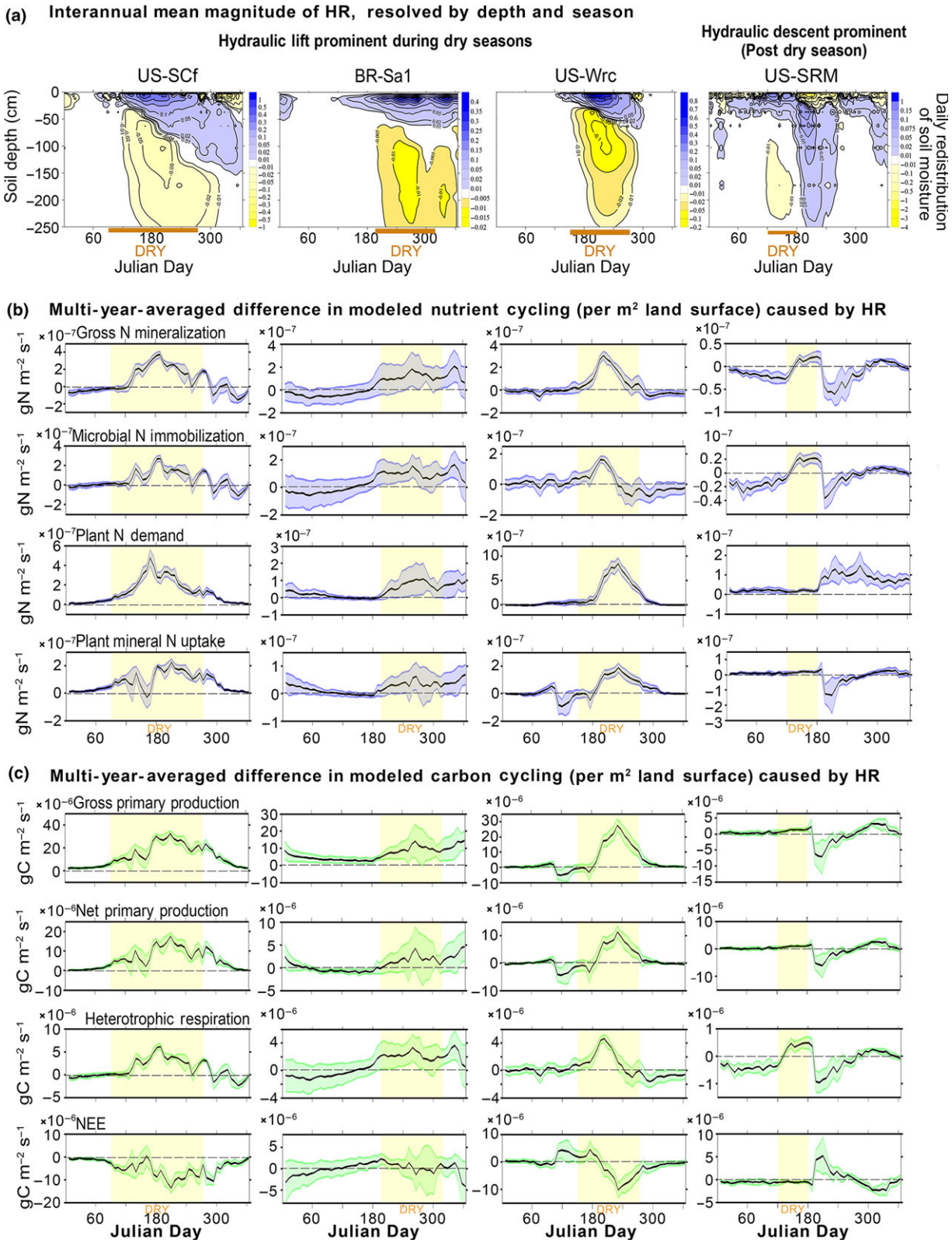

FIGURE 2 Modeled gains and losses of water within the soil column caused by HR, over time and with depth, and associated plant and soil microbial response. Weekly data were averaged across all modeled years. Data are arranged in columns by site. (a) Contour plots of multi-year averaged instantaneous HR (simulated using CLM4.5+HR) show gains and losses of water (quantified as volumetric soil water content, in %) at different depths within soil columns. Blue and gold shading indicate times and soil depths where water is gained (blue) or lost (gold) through the action of HR alone. (b) and (c) Multi-year averaged differences in modeled nutrient (b) and carbon (c) cycling (per m^2 land surface) caused by cumulative effects of HR. Yellow-shaded blocks in (b) and (c) mark dry periods. Interannual means are plotted in black; interannual standard errors are shown with blue (N-processes) or green (C-processes) shading

TABLE 5 Modeled annual, dry season NEE, and wet season NEE (gC/(m^2 s)), at all four Ameriflux sites (1 gC/(m^2 s) ≈ 83 × 10^3 μmol CO_2 m^{-2} s^{-1})

	Annual NEE		Dry season NEE		Wet season NEE	
	CLM4.5noHR	CLM4.5+HR	CLM4.5noHR	CLM4.5+HR	CLM4.5noHR	CLM4.5+HR
US-SCf	4.97E-06	0.32E-06	−6.35E-06	−12.7E-06	11.3E-06	13.0E-06
BR-Sa1	−2.00E-06	−1.99E-06	−8.39E-06	−7.91E-06	6.39E-06	5.92E-06
US-Wrc	0.57E-06	−0.23E-06	−11.3E-06	−13.6E-06	11.9E-06	13.4E-06
US-SRM	−0.77E-06	−0.92E-06	1.89E-06	1.35E-06	−2.66E-06	−2.27E-06

CLM4.5 hybrid model indicated restriction of GPP by downward HR was caused more by plants than microbes. After that short window, however, modeled GPP dropped, and the CLM4.5hybrid (green) and CLM4.5noHR (red) traces became indistinguishable, indicating the further depression of realized GPP in the CLM4.5+HR case (blue) was driven through the microbial pathway, likely via reduced gross mineralization and nutrient availability (Figure 4b).

3.5 | Incidence and spread of fire

Within the CLM4.5 fire module (Li, Zeng et al., 2012; Li et al., 2013; Oleson et al., 2013), the simulated fuel load (combined aboveground vegetation, coarse woody debris, and litter) increased with HR at all four sites (Figure 3), suggesting HR might intensify fire. However, strong upward HR also increased surface soil volumetric water content during fire-prone dry seasons (Figures 2a, S6b and S5a). In CLM4.5, increased root zone soil wetness (which in the field would reflect water content in vegetation) suppresses fire spread.

Figure 5 shows interacting effects of fire and HR on CO_2 fluxes to the atmosphere (Figure 5a) and on vegetation pools (Figure 5b), over multiple years at each site. Uppermost panels of Figure 5a show NEE modeled without HR. In each panel, the dark red trace shows NEE with the fire module engaged; the light red trace shows NEE without the fire module engaged. Where these traces diverge, that is, where inclusion of the fire module drove increased CO_2 release to the atmosphere, the area between the two modeling traces is filled with orange. Without HR, fire was predicted to occur at all four sites: annually at mediterranean US-SCf and semi-arid US-SRM during dry seasons, during the 2009 drought at BR-Sa1, and sporadically at US-Wrc. In lower panels of Figure 5a, HR is included in the modeling; traces are colored blue and grey, for simulations where fire is not (blue) and is (grey) included. Again, fire-driven increases in CO_2 release to the atmosphere are colored orange. Inclusion of HR in CLM4.5 resulted in reduced annual fire-driven CO_2 emissions at US-SCf, and practically no fire at BR-Sa1 and US-Wrc. Although HR slightly decreased fire counts and fuel combustibility (Figure S7), the most dramatic effect of HR was on the reduced spread of any fire that was ignited. Reduced fire spread, as calculated by CLM4.5, resulted dominantly from an increase in root zone soil wetness and associated fuel wetness (Figure S7). At US-SRM, fire-induced emission of CO_2 was not dramatically changed by inclusion of HR in CLM4.5 because in that ecosystem HR dominantly occurs during the rainy season as hydraulic descent.

Model spinup for thousands of years had included HR but no fire. At all sites, fire in the absence of HR (labeled noHR+fire, Figure 5b) notably reduced vegetation pools over time, relative to the initial spinup conditions.

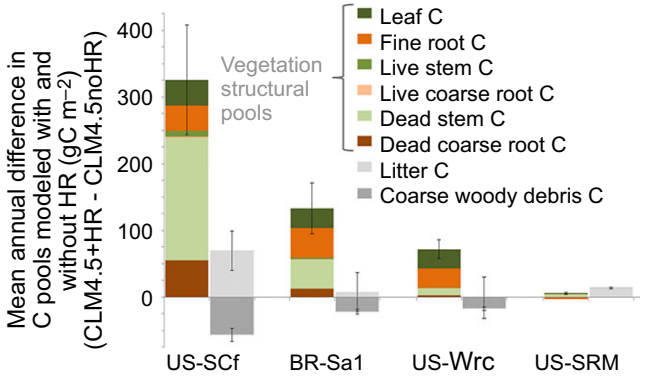

FIGURE 3 Interannual mean (±*SE*) difference in various carbon pools modeled using CLM4.5+HR and CLM4.5noHR

4 | DISCUSSION

Combined measurement and modeling incorporating HR at the Washington, California, Arizona, and Brazilian AmeriFlux sites led to three major conclusions.

First, incorporating HR into CLM4.5 improved model predictions of water, energy, and carbon fluxes measured at tropical and temperate sites with seasonally dry climate. This improvement does not depend on whether upward HR during dry seasons or downward HR during rainy seasons was dominant.

Second, modeled plant productivity and microbial activities were stimulated by upward HR, and diminished by downward HR, relative to the noHR simulations. However, overall plant nutrient demand stimulated by HR could outstrip stimulation of nutrient supply, heightening nutrient limitation, and therefore curtailing the magnitude of increase in realized GPP.

Third, the most potent effect of upward HR on ecosystem carbon release to the atmosphere was via suppression of fire in the model. Surprisingly, though HR increased modeled fuel availability in all four ecosystems, strong upward HR at US-SCf, BR-Sa1, and US-Wrc significantly diminished the modeled spread of fires during dry seasons. (At US-SRM, HR was dominantly downward during the rainy season and had little effect on fire.)

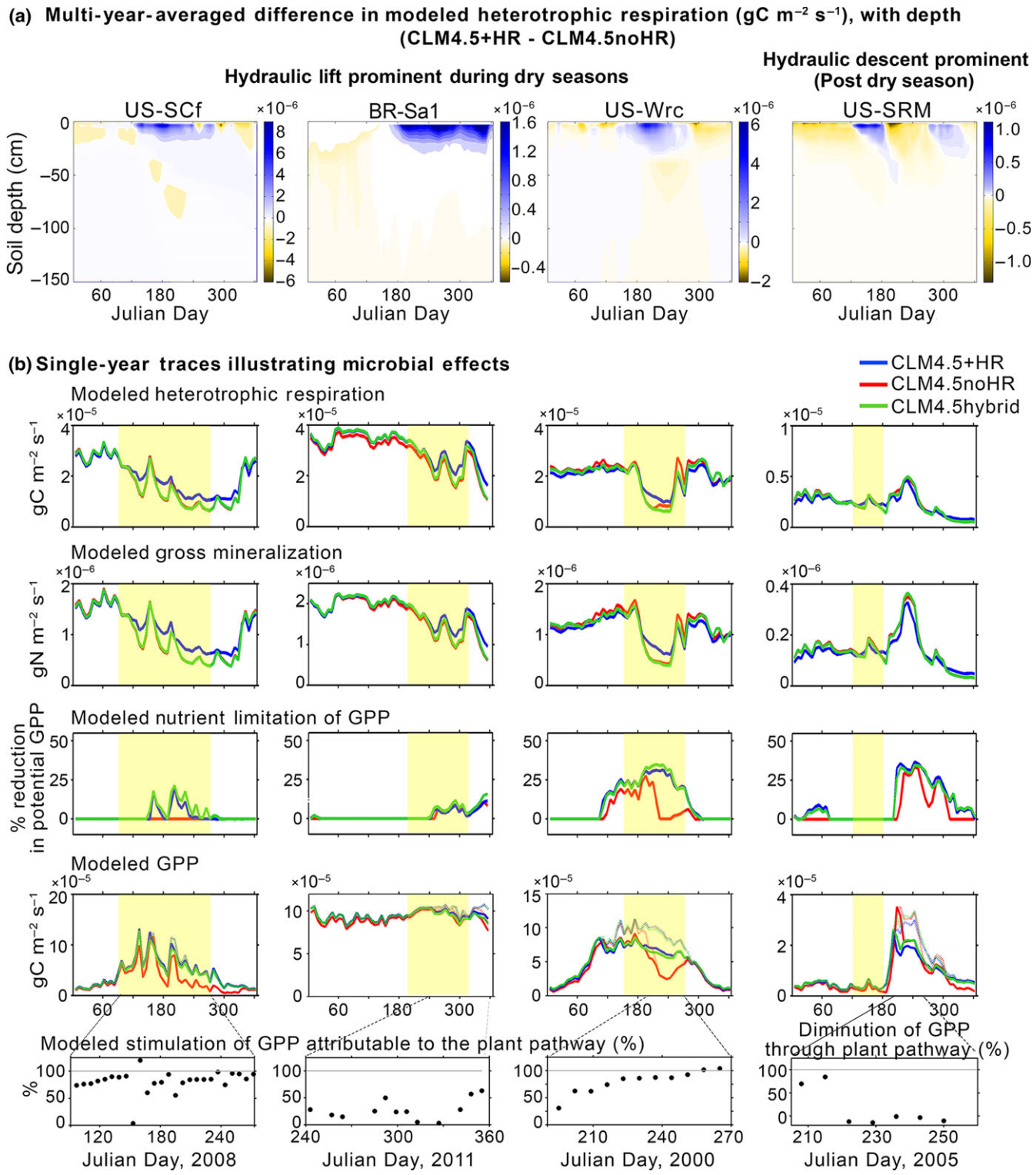

FIGURE 4 Differences in modeled heterotrophic respiration caused by HR, over time and with depth, and concomitant development of nutrient limitation of GPP. (a) Contour plots of multi-year-averaged differences in modeled heterotrophic respiration driven by HR, as a function of soil depth. Weekly data were averaged across all modeled years. Blue shading indicates times and soil depths when heterotrophic respiration is higher in the CLM4.5+HR case than in the CLM4.5noHR case. Gold shading indicates soil depths and times when heterotrophic respiration is lower in the CLM4.5+HR than in the CLM4.5noHR case. (b) Comparison of microbial processes (heterotrophic respiration and gross mineralization), and downregulation of modeled GPP by nutrient limitation, during a single year at each site, modeled using CLM4.5+HR (blue), CLM4.5hybrid (green), and CLM4.5noHR (red) approaches. Data are arranged in columns by site. Yellow-shaded blocks mark dry periods

These findings provide a predictive framework for how HR influences linked hydrological and biogeochemical processes in seasonally dry ecosystems. When hydraulic descent is dominant, downward HR is predicted to reduce rainy season gross mineralization, heterotrophic respiration, GPP, and NPP relative to rates if HR did not occur. Discussion of downward HR in the literature has most often emphasized seasonal deep water storage (e.g., Ryel et al., 2003), and largely has not considered such biogeochemical consequences of water redistribution away from upper soil layers where detritus and root mass are concentrated. Minimal interaction of downward HR with the spread of fire is expected, since strong downward HR during rain does not coincide with the fire season. When upward HR is strong during dry seasons, HR is predicted to increase gross mineralization, heterotrophic respiration, GPP, and NPP, and may notably reduce the spread of dry season fire.

Within this framework, the dominance and timing of upward vs downward HR is predictable from total annual precipitation and the timing of its fall during the year. At the highest rainfall sites US-Wrc and BR-Sa1, the soil column was deeply recharged with water during each rainy season, poising the system for upward HR during the subsequent dry season. Since deep soil layers were not extensively depleted during the dry season, the gradient of soil water potential was relatively weak for downward HR when rains returned. At US-SCf, total annual rainfall was intermediate, and upward HR depleted deep soil moisture during the very long dry period. When rains returned, the strong water potential gradient from surface to deep soil briefly drove hydraulic descent, replenishing deep soil moisture (Fellows & Goulden, 2013). At the driest site US-SRM, overall rainfall was so limited that soil was neither deeply nor completely saturated during the rainy season. Two-thirds of the annual rain fell during the 80 days after the end of the dry season, spurring notable downward HR to dry, deep soil, but not saturating it (Figures 2a and S6b). Upward HR during the subsequent dry season was therefore limited.

From a theoretical perspective, inclusion of HR in CLM4.5 improves the hydrologic realism of the model, and this was supported by improved match of predicted to measured Bowen ratio, ET, and NEE at the four ecologically diverse sites examined here. Several other studies have noted similar improvements, using HR embedded in CLM4.5 (Fu et al., 2016; examining ET and Bowen ratio at eight AmeriFlux sites) and other modeling approaches (Domec et al., 2010; Luo et al., 2013; examining ET, NEE, and GPP). The impact of including HR within models, however, may not always manifest as an immediate reduction in model biases for all variables. For example, Baker et al. (2009) used the Simple Biosphere Model (SiB3) to examine the effects of HR at Tapajos km83 in Brazil and found that including HR did not resolve a mismatch between measured and modeled dynamics in NEE. Tang, Riley, and Niu (2015) embedded Amenu and Kumar's (2008) mathematical representation of HR in CLM4.5 and applied it globally without site-specific meteorological forcing or local information. They found including HR could improve simulation of ET north of 20°N latitude, but not in the tropics.

To test the sensitivity of our model to the HR formulation included in CLM4.5, we substituted Amenu and Kumar's (2008) formulation into CLM4.5, to replace the Ryel et al. (2002) formulation. We parameterized radial and axial specific conductivities of root systems (required in the Amenu and Kumar formulation) in the same way as Tang et al. (2015). Driving the model with site-specific meteorological forcing and other parameters as described for our other simulations, we tested the model at both BR-Sa1 (Brazilian tropics) and US-SCf (California) sites. Unlike Tang et al. (2015) we found improved prediction of ET at both the tropical and the temperate sites. (RMSE at US-SCf was 0.82, and at BR-Sa1 was 0.28, both smaller than the RMSE in the noHR case included in Table 3. Taylor plots comparing model outputs are shown in Figure S8.) The contrast between our results using Amenu and Kumar's formulation and those of Tang et al. (2015) serve as a reminder that inclusion of HR cannot (and is not meant to) compensate for errors caused by imperfect meteorological forcing, deficiencies in model structure, or insufficient calibration of model parameters unrelated to the representation of HR (as also discussed by Tang et al., 2015).

Although many modeled carbon pools and flux rates compare reasonably well with measurements from the sites we studied, there were exceptions. At the very dry site US-SRM, modeled LAI exhibited multiple leaf flushes and losses annually, so was instead specified from site measurements in our simulations. Modeled SOC pools at BR-Sa1 were larger than measured pools; this tendency is a known bias in CLM4.5 with Century-based soil carbon pool kinetics (Koven et al., 2013). But, for example, calculation of microbial immobilization of nutrients in CLM4.5 is not directly affected by soil moisture, thus uncoupling effects of HR on microbial uptake of nutrients from microbe-controlled nitrogen transformations in soil. It is challenging to test the multi-year N pool and process rates produced by CLM4.5 at these AmeriFlux sites; time courses of nitrogen processing rates or pool sizes in soils do not exist at the four focal sites we studied. Though such datasets would be very useful for model testing they are generally very rare. Still, a few pieces of nitrogen pool and process data are available and can be used for spot comparisons. Yang, Ryals, Cusack, and Silver (2017) quantified nitrate pools in 0–10 cm soil cores at five California forested sites, one site being the James Reserve where US-SCf is located. They found average soil nitrate pools of approximately 0.2 mg/kg_{soil}. The averaged CLM4.5-modeled value for spring at US-SCf (from 0 to 9 cm depth) was 0.11 mg/kg_{soil}. Durigan et al. (2017) measured ~4,500 gN/m^2 in surface soil (0–30 cm) in undisturbed forest, Santarem, Brazil; CLM4.5 output from BR-Sa1 (also in Santarem) was 1,245 gN/m^2 (for 0–39 cm soil depth). For US-Wrc, Binkley, Sollins, Bell, Sachs, and Myrold (1992) estimated annual conifer nitrogen uptake at the Wind River Experimental Forest to be in the range of 5 kg ha^{-1} $year^{-1}$ (based on estimates of annual biomass production and the nitrogen concentration of various tissue types), translating to 0.2×10^{-7} gN m^{-2} s^{-1}. The CLM4.5-modeled annual plant N uptake (for all plants at US-Wrc) was ~3 gN m^{-2} s^{-1}. At US-SRM, R. Scott (*unpubl.*) estimated site N pools in soil given measured N pools under bare soil, mesquite, and grass: 0–10,10–20, 20–50, and 50–100 cm depths had estimated 73, 50, 118, and 177 gN m^{-2} s^{-1}. Modeled layers 0–16.6, 16.6–28.9, 28.9–83, 83–138 cm depths held 65,

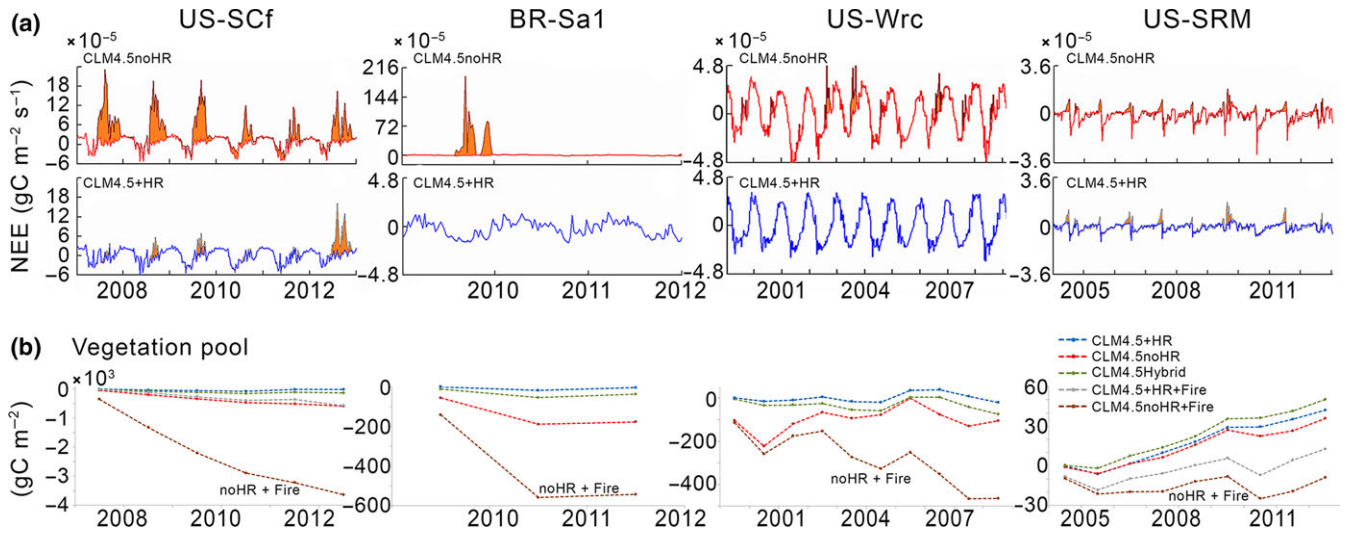

FIGURE 5 Interacting effects of HR and fire. (a) Weekly averaged modeled NEE, when modeled HR is not (upper panels) or is (lower panels) included in CLM4.5. In each panel, modeling runs with and without fire are both graphed; fire-induced CO_2 release to the atmosphere is indicated by orange fill between the two traces. (b) Mean annual size of the vegetation structural carbon pool in all simulations, over time, relative to the initial pool size after spinup of CLM4.5+HR without fire

31, 88, 70 gN/m^2. Overall, though match is not perfect, the modeled values for spot-measured nutrient pools and fluxes are reasonably similar, joining water and carbon pools and fluxes where more data are available for comparison (Figures S3 and S4; Tables 4, S2).

Overall seasonal dynamics in measured NEE were captured appropriately by CLM4.5 with and without HR. However, at US-SCf (and to a lesser extent at US-Wrc), a substantial annual period of winter CO_2 efflux to the atmosphere was predicted by CLM4.5, but not observed (Figure S4). Nighttime NEE was likely underestimated by tower observations at US-SCf, as has been observed elsewhere (Miller et al., 2004), even when calm nights were scrubbed and data gap-filled. Also, modeled winter production in CLM4.5 may have been over-sensitive to cold temperatures; photosynthetic CO_2 uptake has been observed to remain relatively constant as temperatures drop from 15 to as low as 8°C at UC-SCf (Fellows & Goulden, 2013), and conifers in the Pacific Northwest conduct substantial photosynthesis in deep winter (Waring & Franklin, 1979).

Because CLM4.5 is designed for coupling with earth system models at the regional and global scales, mathematical representations of ecosystem processes included are simpler than those in stand- or landscape-scale ecological models. The comparisons of model output and measurements included above are not meant to provide a rigorous test of CLM4.5 as a detailed ecological model. Rather, the comparisons of modeled output and measurements indicate that, overall, CLM4.5 can predict process rates and pools fairly well, and in that capacity the model provides a very useful testbed for broad investigation of system-scale ideas. The idea that upward HR can affect ecosystem function via soil microbial activities has long been in the literature (Aanderud & Richards, 2009; Caldwell et al., 1998; Cardon et al., 2013; Querejeta, Egerton-Warburton, & Allen, 2009). Is the alteration of microbial activity by HR large enough to be ecologically relevant in very diverse (yet seasonally dry) ecosystems? Empirical data quantifying HR's effects on nutrient cycling in the field are scarce (e.g., Cardon et al., 2013), but relevance is suggested here by the modeled stimulation (during upward HR) and diminution (during downward HR) of plant productivity via both plant and microbial pathways.

Relevance is also supported by literature indicating that productivity of many seasonally dry ecosystems can be limited by nutrients as well as water. For example, in northern Utah sagebrush steppe, primary production is limited by both water and nitrogen, and nutrient cycling stimulated by upward HR in late summer enables substantially more uptake of nitrogen by sagebrush (Cardon et al., 2013). Primary production at US-Wrc can be nitrogen limited (Binkley, 2003; Klopatek, Barry, & Johnson, 2006), and production at BR-Sa1 can be phosphorus limited, with strong recycling of organic phosphorus catalyzed by enzymes from roots and microbes (Davidson et al., 2007; Keller, Kaplan, Wofsy, & Maria Da Costa, 1988; Malhi et al., 2009; McGroddy, Silver, & de Oliveira, 2004). (Though CLM4.5 has only nitrogen limitation coded into the control of GPP, the stimulation of microbial activity by upward HR likely could, in the field, affect bacterial and fungal microbial activities improving phosphorus as well as nitrogen availability.) At US-SCf, the extent of soil nutrient limitation of primary production has not been assessed, but oak forests in Mediterranean climate on multiple continents tend to be nutrient as well as water limited (Rodà, Mayor, Sabaté, & Diego, 1999). And at semi-arid US-SRM, young mesquite (*Prosopis glandulosa*), a dominant at the site, is known to expend energy to obtain most of its nitrogen from N-fixing bacterial symbionts when young, but more fertile patches with higher soil nitrogen content can develop around the mesquite trees as they age (Geesing, Felker, & Bingham, 2000). Still, the constraint on modeled GPP (relative to the noHR case) associated with downward HR is largely driven in CLM4.5+HR by nutrient limitation (Figure 4b).

The largest modeled effect of HR on NEE, however, was via a surprising suppression of the spread of fire. At all sites modeled

here, the simulated fuel load increased with HR, but inclusion of HR in the model at US-SCf, BR-Sa1, and US-Wrc resulted in reduced spread of fire (and associated CO_2 fluxes to the atmosphere) relative to the prediction without HR. We can speculate on field mechanisms that would contribute to reduced fire spread when upward HR is occurring. A better hydrated overstory, for example, could lead to more humid and calm subcanopy, and thus improved surface fuel resistance to burning. Increased litter, understory, and/or ground cover moisture with HR could also lead to lower understory fire intensity, less damage to phloem, and reduced tree mortality. Although the prognostic fire module in CLM4.5 does not delve into plant physiological detail, it does take into account different PFTs, and uses variables related to the field mechanisms noted above (Li, Wang et al., 2012; Li, Zeng et al., 2012). Burned area is determined by fire count and spread, and fire count and spread are complex functions of multiple environmental and human social variables. Fire count is simulated as a function of both fuel availability (increased by HR) and fuel combustibility (among other variables); combustibility is reduced by high relative humidity and volumetric soil moisture, both potentially increased by HR. However, fire counts differed only minimally in the CLM4.5+HR and CLM4.5noHR simulations (Figure S7). Fire spread, however, was notably diminished by HR. The average spread area of each fire is simulated as a function of wind speed, relative humidity, and root zone soil wetness (influencing canopy moisture content). The parameterization of these dependencies makes use of several threshold values that are critical for determining fire occurrence and emission, including for example a relative humidity threshold of 70% above which fuel is considered not combustible and a root zone soil saturation threshold of 70% above which fire would not spread. While the CLM4.5 fire module has been tested against the satellite-based Global Fire Emission Database 3 (Li, Zeng et al., 2012; Li et al., 2013; Oleson et al., 2013), the parameterizations are certainly hindered by the lack of empirical data especially on the values of those thresholds. The HR-induced reduction in fire spread found in this study was primarily through increasing the root zone soil wetness above 70% saturation. Model results are therefore sensitive to uncertainties related to this threshold and to other thresholds used in the fire module as well, especially given the simulated increase in fuel load caused by HR. Addressing these uncertainties requires field experiments and/or collection of empirical data on the several critical parameters used in the fire module.

Overall, our work illustrates that understanding the larger importance of HR in seasonally dry ecosystems requires moving beyond considering only the direct effects of HR on stomatal conductance, evapotranspiration, and photosynthesis (the plant pathway). Modeling indicates both upward and downward HR can affect the balance of nutrient supply and demand, and CO_2 fixation and respiration, all of which interact as major determinants of system productivity and exchange of CO_2 with the atmosphere. In many seasonally dry ecosystems, fire has been a dominant ecological force historically, and intensification of soil drought and altered precipitation regimes are expected in the future. HR may play an increasingly important role mitigating development of extreme soil water potential gradients and associated limitations on plant and soil microbial activities, and may curtail the spread of fire in seasonally dry ecosystems.

ACKNOWLEDGEMENTS

This research was supported by the Office of Science (BER), U.S. Department of Energy (DE-SC0008182 ER65389 to ZGC and GW). Thanks to Steven C. Wofsy for his contributions to the BR-Sa1 site data. Funding for AmeriFlux sites was provided by the U.S. Department of Energy's Office of Science.

CONFLICT OF INTEREST

The authors declare no conflict of interest.

AUTHOR CONTRIBUTIONS

CF and GW performed the modeling. CF, GW, and ZGC analyzed the modeling output, incorporated the AmeriFlux data, and wrote the paper. KB, MLG, SRS, and RLS contributed AmeriFlux data and commented on the manuscript.

ORCID

Congsheng Fu http://orcid.org/0000-0002-9128-7400
Guiling Wang http://orcid.org/0000-0002-9744-2563
Zoe G. Cardon http://orcid.org/0000-0001-8725-7842

REFERENCES

Aanderud, Z. T., & Richards, J. H. (2009). Hydraulic redistribution may stimulate decomposition. *Biogeochemistry*, *95*, 323–333. https://doi.org/10.1007/s10533-009-9339-3

Amenu, G. G., & Kumar, P. (2008). A model for hydraulic redistribution incorporating coupled soil-root moisture transport. *Hydrology and Earth System Sciences*, *12*, 55–74. https://doi.org/10.5194/hess-12-55-2008

Anderson, R. G., & Goulden, M. L. (2011). Relationships between climate, vegetation, and energy exchange across a montane gradient. *Journal of Geophysical Research: Biogeosciences*, *116*, G01026.

Aragão, L. E. O. C., Shimabukuro, Y. E., Espírito Santo, F. D. B., & Williams, M. (2005). Landscape pattern and spatial variability of leaf area index in Eastern Amazonia. *Forest Ecology and Management*, *211*, 240–256. https://doi.org/10.1016/j.foreco.2005.02.062

Baker, I. T., Prihodko, L., Denning, A. S., Goulden, M., Miller, S., & Da Rocha, H. R. (2009). Seasonal drought stress in the amazon: Reconciling models and observations. *Journal of Geophysical Research: Biogeosciences*, *113*, G00B01.

Barron-Gafford, G. A., Sanchez-Cañete, E. P., Minor, R. L., Hendryx, S. M., Lee, E., Sutter, L. F., … Scott, R. L. (2017). Impacts of hydraulic redistribution on grass–tree competition vs facilitation in a semi-arid savanna. *New Phytologist*, *215*, 1451–1461. https://doi.org/10.1111/nph.14693

Binkley, D. (2003). Seven decades of stand development in mixed and pure stands of conifers and nitrogen-fixing red alder. *Canadian Journal of Forest Research*, *33*, 2274–2279. https://doi.org/10.1139/x03-158

Binkley, D., Sollins, P., Bell, R., Sachs, D., & Myrold, D. (1992). Biogeochemistry of adjacent conifer and alder-conifer stands. *Ecology*, *73*, 2022–2033. https://doi.org/10.2307/1941452

Brooks, J. R., Meinzer, F. C., Coulombe, R., & Gregg, J. (2002). Hydraulic redistribution of soil water during summer drought in two contrasting Pacific Northwest coniferous forests. *Tree Physiology*, *22*, 1107–1117. https://doi.org/10.1093/treephys/22.15-16.1107

Caldwell, M. M., Dawson, T. E., & Richards, J. H. (1998). Hydraulic lift: Consequences of water efflux from the roots of plants. *Oecologia*, *113*, 151–161. https://doi.org/10.1007/s004420050363

Cardon, Z. G., Stark, J. M., Herron, P. M., & Rasmussen, J. A. (2013). Sagebrush carrying out hydraulic lift enhances surface soil nitrogen cycling and nitrogen uptake into inflorescences. *Proceedings of the National Academy of Sciences*, *110*, 18988–18993. https://doi.org/10.1073/pnas.1311314110

Chambers, J. Q., Tribuzy, E. S., Toledo, L. C., Crispim, B. F., Santos, J., Araújo, A. C., … Trumbore, E. (2014). Respiration from a tropical forest ecosystem : Partitioning of sources and low carbon use efficiency. *Ecological Applications*, *14*(4), S72–S88.

Clapp, R. B., & Hornberger, G. M. (1978). Empirical equations for some soil hydraulic properties. *Water Resources Research*, *14*, 601–604. https://doi.org/10.1029/WR014i004p00601

Davidson, E. A., de Carvalho, C. J. R., Figueira, A. M., Ishida, F. Y., Ometto, J. P. H. B., Nardoto, G. B., … Martinelli, L. A. (2007). Recuperation of nitrogen cycling in Amazonian forests following agricultural abandonment. *Nature*, *447*, 995–998. https://doi.org/10.1038/nature05900

Domec, J. C., King, J. S., Noormets, A., Treasure, E., Gavazzi, M. J., Sun, G., & McNulty, S. G. (2010). Hydraulic redistribution of soil water by roots affects whole-stand evapotranspiration and net ecosystem carbon exchange. *New Phytologist*, *187*, 171–183. https://doi.org/10.1111/j.1469-8137.2010.03245.x

Durigan, M. R., Cherubin, M. R., de Camargo, P. B., Ferreira, J. N., Berenguer, E., Gardner, T. A., … Cerri, C. E. P. (2017). Soil organic matter responses to anthropogenic forest disturbance and land use change in the Eastern Brazilian Amazon. *Sustainability*, *9*, 379. https://doi.org/10.3390/su9030379

Falk, M., Wharton, S., Schroeder, M., Ustin, S. L., & Paw U, K. T. (2008). Flux partitioning in an old-growth forest: Seasonal and interannual dynamics. *Tree Physiology*, *28*, 509–520. https://doi.org/10.1093/treephys/28.4.509

Fellows, A. W., & Goulden, M. L. (2013). Controls on gross production by a semiarid forest growing near its warm and dry ecotonal limit. *Agricultural and Forest Meteorology*, *169*, 51–60. https://doi.org/10.1016/j.agrformet.2012.10.001

Frank, D., Reichstein, M., Bahn, M., Thonicke, K., Frank, D., Mahecha, M. D., … Zscheischler, J. (2015). Effects of climate extremes on the terrestrial carbon cycle: Concepts, processes and potential future impacts. *Global Change Biology*, *21*, 2861–2880. https://doi.org/10.1111/gcb.12916

Fu, C., Wang, G., Goulden, M. L., Scott, R. L., Bible, K., & Cardon, Z. G. (2016). Combined measurement and modeling of the hydrological impact of hydraulic redistribution using CLM4.5 at eight AmeriFlux sites. *Hydrology and Earth System Sciences*, *20*, 2001–2018. https://doi.org/10.5194/hess-20-2001-2016

Geesing, D., Felker, P., & Bingham, R. L. (2000). Influence of mesquite (*Prosopis glandulosa*) on soil nitrogen and carbon development: Implications for global carbon sequestration. *Journal of Arid Environments*, *46*, 157–180. https://doi.org/10.1006/jare.2000.0661

Grant, R. F., Hutyra, L. R., De Oliveira, R. C., Munger, J. W., Saleska, S. R., & Wofsy, S. C. (2009). Modeling the carbon balance of Amazonian rain forests : Resolving ecological controls on net ecosystem productivity. *Ecological Monographs*, *79*, 445–463. https://doi.org/10.1890/08-0074.1

Harmon, M., Bible, K., Ryan, M., Shaw, D., Chen, H., Klopatek, J., & Li, X. (2004). Production, respiration, and overall carbon balance in an old-growth *Pseudotsuga-Tsuga* forest ecosystem. *Ecosystems*, *7*, 498–512.

Hutyra, L. R., Munger, J. W., Hammond-Pyle, E., Saleska, S. R., Restrepo-Coupe, N., Daube, B. C., … Wofsy, S. C. (2008). Resolving systematic errors in estimates of net ecosystem exchange of CO_2 and ecosystem respiration in a tropical forest biome. *Agricultural and Forest Meteorology*, *148*, 1266–1279. https://doi.org/10.1016/j.agrformet.2008.03.007

Ivanov, V. Y., Hutyra, L. R., Wofsy, S. C., Munger, J. W., Saleska, S. R., De Oliveira, R. C., & De Camargo, P. B. (2012). Root niche separation can explain avoidance of seasonal drought stress and vulnerability of overstory trees to extended drought in a mature Amazonian forest. *Water Resources Research*, *48*, W12507.

Jackson, R. B., Canadell, J., Ehleringer, J. R., Mooney, H. A., Sala, O. E., & Schulze, E. D. (1996). A global analysis of root distributions for terrestrial biomes. *Oecologia*, *108*, 389–411. https://doi.org/10.1007/BF00333714

Keller, M., Kaplan, W., Wofsy, S., & Maria Da Costa, J. (1988). Emissions of N_2O from tropical forest soils: Response to fertilization with NH_4^+, NO_3^-, and PO_4^{3-}. *Journal of Geophysical Research*, *93*, 1600–1604. https://doi.org/10.1029/JD093iD02p01600

Kitajima, K., Allen, M. F., & Goulden, M. L. (2013). Contribution of hydraulically lifted deep moisture to the water budget in a Southern California mixed forest. *Journal of Geophysical Research: Biogeosciences*, *118*, 1561–1572.

Klopatek, J. M., Barry, M. J., & Johnson, D. W. (2006). Potential canopy interception of nitrogen in the Pacific Northwest, USA. *Forest Ecology and Management*, *234*, 344–354. https://doi.org/10.1016/j.foreco.2006.07.019

Koven, C. D., Riley, W. J., Subin, Z. M., Tang, J. Y., Torn, M. S., Collins, W. D., … Swenson, S. C. (2013). The effect of vertically resolved soil biogeochemistry and alternate soil C and N models on C dynamics of CLM4. *Biogeosciences*, *10*, 7109–7131. https://doi.org/10.5194/bg-10-7109-2013

Lee, J.-E., Oliveira, R. S., Dawson, T. E., & Fung, I. (2005). Root functioning modifies seasonal climate. *Proceedings of the National Academy of Sciences of the United States of America*, *102*, 17576–17581. https://doi.org/10.1073/pnas.0508785102

Li, F., Levis, S., & Ward, D. S. (2013). Quantifying the role of fire in the Earth system - Part 1: Improved global fire modeling in the Community Earth System Model (CESM1). *Biogeosciences*, *10*, 2293–2314. https://doi.org/10.5194/bg-10-2293-2013

Li, L., Wang, Y. P., Yu, Q., Pak, B., Eamus, D., Yan, J., … Baker, I. T. (2012). Improving the responses of the Australian community land surface model (CABLE) to seasonal drought. *Journal of Geophysical Research: Biogeosciences*, *117*, G04002.

Li, F., Zeng, X. D., & Levis, S. (2012). A process-based fire parameterization of intermediate complexity in a dynamic global vegetation model. *Biogeosciences*, *9*, 2761–2780. https://doi.org/10.5194/bg-9-2761-2012

Luo, X., Liang, X., & McCarthy, H. R. (2013). VIC+ for water-limited conditions: A study of biological and hydrological processes and their interactions in soil-plant-atmosphere continuum. *Water Resources Research*, *49*, 7711–7732. https://doi.org/10.1002/2012WR012851

Malhi, Y., Aragão, L. E. O. C., Metcalfe, D. B., Paiva, R., Quesada, C. A., Almeida, S., … Teixeira, L. M. (2009). Comprehensive assessment of carbon productivity, allocation and storage in three Amazonian forests. *Global Change Biology*, *15*, 1255–1274. https://doi.org/10.1111/j.1365-2486.2008.01780.x

McGroddy, M. E., Silver, W. L., & de Oliveira, R. C. (2004). The effect of phosphorus availability on decomposition dynamics in a seasonal lowland Amazonian forest. *Ecosystems*, *7*, 172–179.

Meinzer, F. C., Brooks, J. R., Bucci, S., Goldstein, G., Scholz, F. G., & Warren, J. M. (2004). Converging patterns of uptake and hydraulic redistribution of soil water in contrasting woody vegetation types. *Tree Physiology*, *24*, 919–928. https://doi.org/10.1093/treephys/24.8.919

Miller, S. D., Goulden, M. L., Menton, M. C., Rocha, H. R., Freitas, H. C., Figueira, A. M. S., & Sousa, C. A. D. (2004). Tower-based and biometry-

based measurements of tropical forest carbon balance. *Ecological Applications*, *14*(Supplement), S114–S126. https://doi.org/10.1890/02-6005

Nepstad, D. C., de Carvalho, C. R., Davidson, E. A., Jipp, P. H., Lefebvre, P. A., Negreiros, G. H., … Vieira, S. (1994). The role of deep roots in the hydrological and carbon cycles of Amazonian forests and pastures. *Nature*, *372*, 666–669. https://doi.org/10.1038/372666a0

Neumann, R. B., & Cardon, Z. G. (2012). The magnitude of hydraulic redistribution by plant roots: A review and synthesis of empirical and modeling studies. *New Phytologist*, *194*, 337–352. https://doi.org/10.1111/j.1469-8137.2012.04088.x

Oleson, K. W., Lawrence, D. M., Bonan, G. B., Drewniak, B., Huang, M., Koven, C. D., … Yang, Z.-L. (2013). *Technical description of version 4.5 of the community land model (CLM)*. NCAR Technical Note NCAR/TN-503 + STR (420 p.). National Center for Atmospheric Research, Boulder, CO.

Oliveira, R. S., Dawson, T. E., Burgess, S. S. O., & Nepstad, D. C. (2005). Hydraulic redistribution in three Amazonian trees. *Oecologia*, *145*, 354–363. https://doi.org/10.1007/s00442-005-0108-2

Prieto, I., Armas, C., & Pugnaire, F. I. (2012). Water release through plant roots: New insights into its consequences at the plant and ecosystem level. *New Phytologist*, *193*, 830–841. https://doi.org/10.1111/j.1469-8137.2011.04039.x

Querejeta, J. I., Egerton-Warburton, L. M., & Allen, M. F. (2009). Topographic position modulates the mycorrhizal response of oak trees to interannual rainfall variability. *Ecology*, *90*, 649–662. https://doi.org/10.1890/07-1696.1

Quijano, J. C., & Kumar, P. (2015). Numerical simulations of hydraulic redistribution across climates: The role of the root hydraulic conductivities. *Water Resources Research*, *51*, 8529–8550. https://doi.org/10.1002/2014WR016509

Reich, P. B., Walters, M. B., & Ellsworth, D. S. (1997). From tropics to tundra: Global convergence in plant functioning. *Proceedings of the National Academy of Sciences*, *94*, 13730–13734. https://doi.org/10.1073/pnas.94.25.13730

Richards, J. H., & Caldwell, M. M. (1987). Hydraulic lift: Substantial nocturnal water transport between soil layers by *Artemisia tridentata* roots. *Oecologia*, *73*, 486–489. https://doi.org/10.1007/BF00379405

Richardson, A. D., Anderson, R. S., Arain, M. A., Barr, A. G., Bohrer, G., Chen, G., … Xue, Y. (2012). Terrestrial biosphere models need better representation of vegetation phenology: results from the North American Carbon Program Site Synthesis. *Global Change Biology*, *18*, 566–584. https://doi.org/10.1111/j.1365-2486.2011.02562.x

Rodà, F., Mayor, X., Sabaté, S., & Diego, V. (1999). Water and nutrient limitations to primary production. In F. Rodà, J. Retana, C. A. Gracia & J. Bellot (Eds.), *Ecology of mediterranean evergreen oak forests. Ecological Studies (Analysis and Synthesis)*, vol. *137* (pp. 183–194). Berlin, Heidelberg, Germany: Springer. https://doi.org/10.1007/978-3-642-58618-7

Ryel, R. J., Caldwell, M. M., Leffler, A. J., & Yoder, C. K. (2003). Rapid soil moisture recharge to depth by roots in a stand of *Artemisia tridentata*. *Ecology*, *84*, 757–764. https://doi.org/10.1890/0012-9658(2003)084[0757:RSMRTD]2.0.CO;2

Ryel, R. J., Caldwell, M. M., Yoder, C. K., Or, D., & Leffler, A. (2002). Hydraulic redistribution in a stand of *Artemisia tridentata*: Evaluation of benefits to transpiration assessed with a simulation model. *Oecologia*, *130*, 173–184. https://doi.org/10.1007/s004420100794

Sardans, J., & Peñuelas, J. (2014). Hydraulic redistribution by plants and nutrient stoichiometry: Shifts under global change. *Ecohydrology*, *7*, 1–20. https://doi.org/10.1002/eco.1459

Scott, R. L., Biederman, J. A., Hamerlynck, E. P., & Barron-Gafford, G. A. (2015). The carbon balance pivot point of southwestern U.S. semiarid ecosystems: Insights from the 21st century drought. *Journal of Geophysical Research –Biogeosciences.*, *120*, 2612–2624. https://doi.org/10.1002/2015JG003181

Scott, R. L., Cable, W. L., & Hultine, K. R. (2008). The ecohydrologic significance of hydraulic redistribution in a semiarid savanna. *Water Resources Research*, *44*, W02440.

Scott, R. L., Jenerette, G. D., Potts, D. L., & Huxman, T. E. (2009). Effects of seasonal drought on net carbon dioxide exchange from a woody-plant-encroached semiarid grassland. *Journal of Geophysical Research: Biogeosciences*, *114*, G04004.

Shaw, D. C., Franklin, J. F., Bible, K., Klopatek, J., Freeman, E., Greene, S., … Klopat, J. (2004). Ecological setting of the Wind River old-growth forest. *Ecosystems*, *7*, 427–439.

Tang, J., Riley, W. J., & Niu, J. (2015). Incorporating root hydraulic redistribution in CLM4.5: Effects on predicted site and global evapotranspiration, soil moisture, and water storage. *Journal of Advances in Modeling Earth Systems*, *7*, 1828–1848. https://doi.org/10.1002/2015MS000484

Taylor, K. E. (2001). Summarizing multiple aspects of model performance in a single diagram. *Journal of Geophysical Research*, *106*(D7), 7183–7192. https://doi.org/10.1029/2000JD900719

Thornton, P. E., Law, B. E., Gholz, H. L., Clark, K. L., Falge, E., Ellsworth, D. S., … Sparks, J. P. (2002). Modeling and measuring the effects of disturbance history and climate on carbon and water budgets in evergreen needleleaf forests. *Agricultural and Forest Meteorology*, *113*, 185–222. https://doi.org/10.1016/S0168-1923(02)00108-9

Wang, G. (2011). Assessing the potential hydrological impacts of hydraulic redistribution in Amazonia using a numerical modeling approach. *Water Resources Research*, *47*, W02528.

Wang, G., Alo, C., Mei, R., & Sun, S. (2011). Droughts, hydraulic redistribution, and their impact on vegetation composition in the Amazon forest. *Plant Ecology*, *212*, 663–673. https://doi.org/10.1007/s11258-010-9860-4

Waring, R. H., & Franklin, J. F. (1979). Evergreen coniferous forests of the Pacific Northwest. *Science*, *204*, 1380–1386. https://doi.org/10.1126/science.204.4400.1380

Warren, J. M., Meinzer, F. C., Brooks, J. R., & Domec, J. C. (2005). Vertical stratification of soil water storage and release dynamics in Pacific Northwest coniferous forests. *Agricultural and Forest Meteorology*, *130*, 39–58. https://doi.org/10.1016/j.agrformet.2005.01.004

Yang, W. H., Ryals, R. A., Cusack, D. F., & Silver, W. L. (2017). Cross-biome assessment of gross soil nitrogen cycling in California ecosystems. *Soil Biology & Biochemistry*, *107*, 144–155. https://doi.org/10.1016/j.soilbio.2017.01.004

Yu, K., & D'Odorico, P. (2015). Hydraulic lift as a determinant of tree-grass coexistence on savannas. *New Phytologist*, *207*, 1038–1051. https://doi.org/10.1111/nph.13431

Zheng, Z., & Wang, G. (2007). Modeling the dynamic root water uptake and its hydrological impact at the Reserva Jaru site in Amazonia. *Journal of Geophysical Research: Biogeosciences*, *112*, G04012.

SUPPORTING INFORMATION

Additional supporting information may be found online in the Supporting Information section at the end of the article.

How to cite this article: Fu C, Wang G, Bible K, et al. Hydraulic redistribution affects modeled carbon cycling via soil microbial activity and suppressed fire. *Glob Change Biol*. 2018;24:3472–3485. https://doi.org/10.1111/gcb.14164